SIMULATION OF WIND TUNNEL FORCES USING MAGNETIC SUSPENSION TECHNOLOGY

R.Ralph Sinno Thomas Price
Department of Civil Engineering
Mississippi State University

Bert Nail Jason Melton
Department of Electrical and Computer Engineering
Mississippi State University
Mississippi State, MS 39762

SUMMARY

Forces experienced by metal roofs under high wind conditions vary as a function of both time and space. Modeling a roof structure subdivided into segments or nodes accommodates spatial variation, for which magnetic suspended actuators are made to generate time-tailored forces equivalent to the wind-induced forces. In this study, each node consists of an induced electromagnetic actuator, an electronic control board, and a load cell for verification of the force produced. Short duration wind gust and the effect of such impulsive loading on a metal roof panel and the overall structural system are poorly incorporated in the present state-of-the-art in structural analysis and design. A full-scale testing facility for metal building roof components, now in operation at Mississippi State University, provides realistic forces that approximate those produced by high velocity winds from wind tunnel models.

INTRODUCTION

High velocity wind on relatively flat roofs of low-rise buildings exerts uplift pressures that are potentially destructive and hazardous to human life. Tests performed in wind tunnels on small modules, 1/50 scale, confirm the dynamic nonuniformity of hurricane wind loadings. Although wind loading is known to be nonuniform and unsteady, uniform static loading is the only currently available method of simulating high velocity wind loading for engineering analysis, design and research.

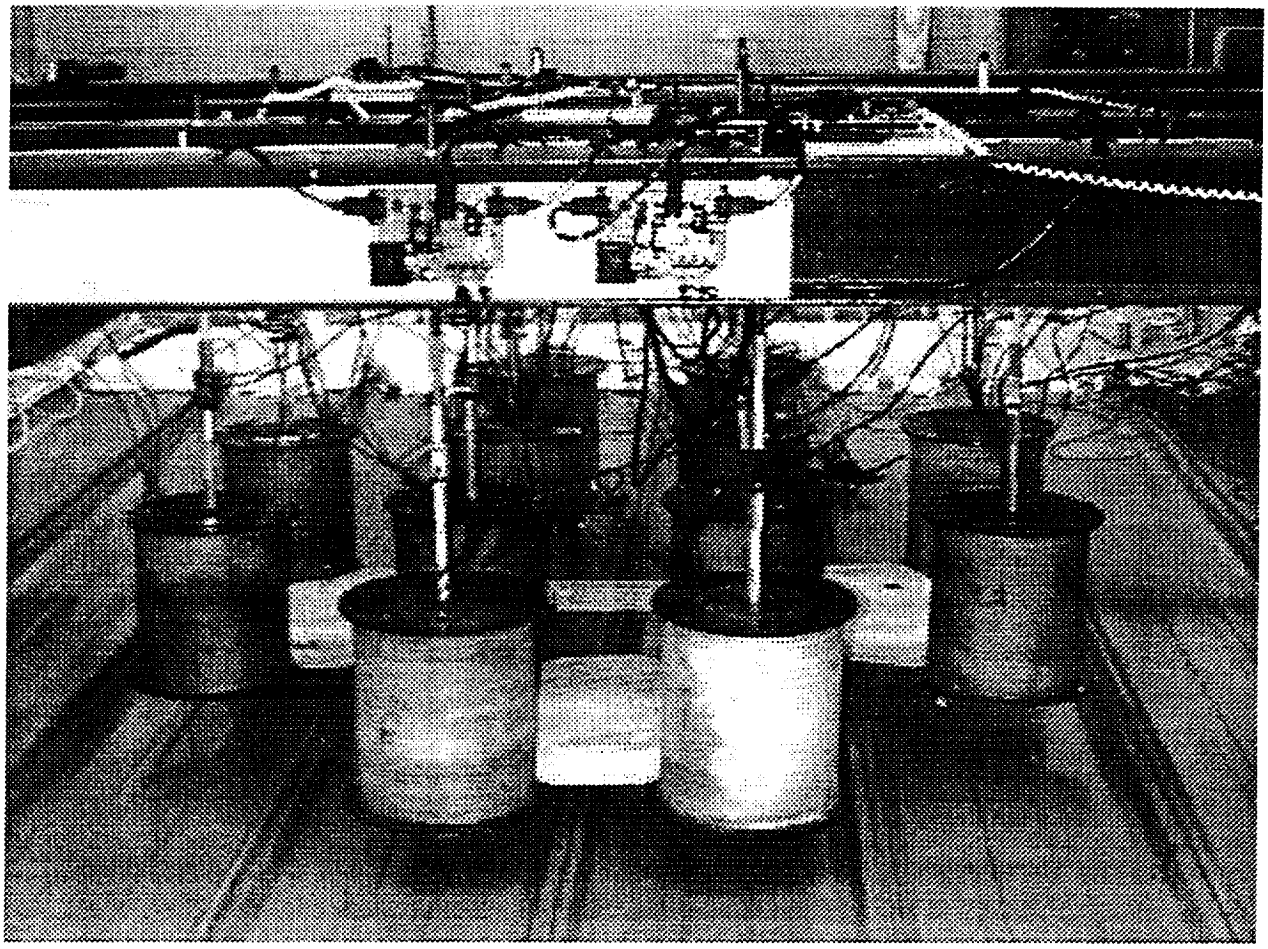

Figure 1. Wind Simulation Test Setup.

Metal building construction is presently the fastest growing segment in the low rise building construction industry. The primary lateral and dynamic loading on these buildings is caused by high velocity wind. The present design procedure of using the uniform uplift forces on metal roofs is highly questionable, and unrealistic from an engineering point of view. Analyzing and designing metal buildings for the true spectrum of dynamic, spatially variable wind loading, as recorded from wind tunnel testing programs, represents a significant advance in the state of knowledge in the metal building industry. The ongoing research at Mississippi State to establish a testing program that utilizes the true wind loadings is expected to open new and exciting options in innovations, analysis and design.

In this research, nonuniform dynamic forces are produced using induced intensive electromagnetic fields. An individually controlled, magnetized grid of nodal points is electronically monitored and controlled to produce dynamic electromagnetic suction forces (Figure 1). The induced electromagnetic forces are then adjusted to any given or randomly generated suite of nonuniform dynamic wind loading. Extensive research on the efficacy and optimization of the induced electromagnetic forces in the grid system has been investigated. Significant technical challenges have been overcome to generate the needed pressure intensity within the time and space criteria imposed by the physics of the underlying problem. The test set-up being developed will be used at a later date

to investigate the failure modes and cause of failure of light gauge metal roofs, and to develop simplified analysis and design procedures to be used by the metal building industry.

BACKGROUND

The effects of wind loading have taken an increasingly important role in the design of metal buildings. The goal is to better prevent loss of life and to lessen property losses. Hurricanes Hugo (1989), Iniki (1992) and Andrew (1992), which struck Puerto Rico and South Carolina; Hawaii; and Southern Florida respectively, demonstrated the importance of considering wind loads in the design and construction of typical metal buildings. Some of the current research areas are probabilistic assessment of wind speeds, translation of wind speeds into loads through wind tunnel testing, validation of this translation through full-scale testing, and documentation of damage and economic assessment of construction techniques. The aim of this type of research is to allow increased testing of building response to this type of load, and to improve the safety and efficiency of building designs [1].

The research presented here involves full-scale testing. Wind load forces generated from wind tunnel testing by the University of Western Ontario [2] are recreated on a full-scale model. A roof testing system based on magnetic actuators and embedded processors has been developed, and is currently operational in a multi-magnet configuration. The system is generating realistic forces such as those experienced by a metal roof structure under high wind velocity conditions. The techniques for controlling the nodes and measuring the results are described herein. The process that is used to calibrate magnetically generated forces and wind tunnel data is especially interesting and is described in some detail. The results for the single magnet configuration are shown and the expansion of the process to account for multiple magnets is presented.

TEST APPARATUS

Forces experienced by a metal roof under high wind conditions vary widely, both as a function of time, and as a function of position. Subdividing a roof structure into segments or nodes (See Figure 1) accommodates positional variation, for which actuators generate time-tailored forces equivalent to the forces of nature. Each node consists of the actuator, an electronic control board for the electromagnet, and a load cell for verification of the force produced. This is shown in Figure 2.

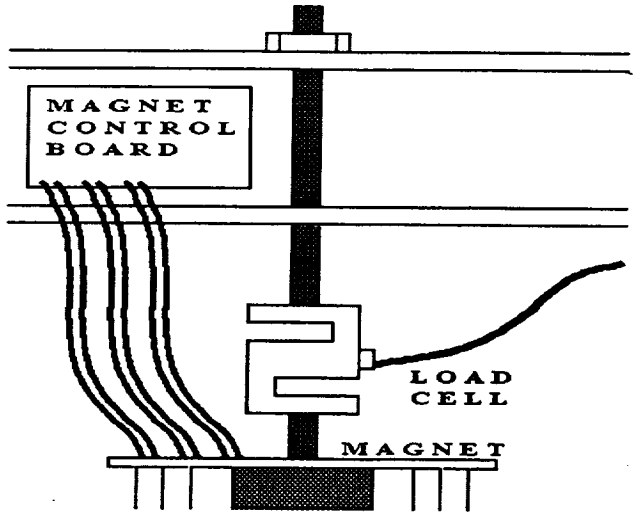

Figure 2. Elements of a Node.

The most noticeable part of each node is the actuator – an electromagnet, which consists of three coils to be powered selectively from a three-phase 208-volt source (Figures 1 and 2). This is also most interesting from a control perspective, since it embodies strong elements of nonlinearly, and cross coupling between neighboring nodes. The electromagnets are approximately 11 inches in diameter and 13 inches high, weigh about 270 pounds, and can exert forces in excess of 300 pounds on a thin sheet of metal at a distance of 1 inch. This does not sound impressive until compared to a commercial lift magnet tested to 14,000 pounds – that magnet only achieved a force of about 30 pounds on a thin sheet at the same distance. Any combination of the three magnet coils can be energized to provide a wide variation of force, with peak power near 4 KW. The control of these closely coupled magnets, highly nonlinear with gap distance, to achieve forces matching the wind tunnel data, is the thrust of this paper.

The completed system is to have 36 nodes, which must be closely synchronized and centrally commanded. Zero crossing detectors on each electronics board are connected to one phase of the AC power, thus establishing 120 Hz pulses as a time base. Each control board groups the time base into frames of 6 pulses, which matches the 20 Hz wind tunnel sampling time.

Simple commands (start, stop, ...) are daisy-chained through optoisolators on each magnet control board as current signals to diminish noise. Phone cables are used for command signal interconnection between nodes for reconfiguration ease. Commands from the central controller are first daisy-chained through beam controller boards, and they relay the information in another daisy chain to the magnet control boards. All units operate from the same time base for synchronization, and any problem in connection is easily noticeable since an entire daisy-chained group will fail. The daisy chain arrangement is shown in Figure 3.

On each magnet control board is a Microchip PIC16F84 8-bit microcontroller, a Microchip 24AA65 I^2C serial eeprom (8k x 8), three Crydom solid state relays and a Harris CA3059 zero-voltage switch used to create the 120 pulses per second time frame. The forces for each $1/20^{th}$ frame are stored in the serial eeprom, which has an identical pin-out for a wide range of memory sizes, for

easy memory upgrade. The solid-state relays allow selected activation of the three-phase magnet windings. The PIC16F84 is the brains of the board, responsible for deciphering commands, retrieving the drive data for the next frame and turning on the appropriate magnet coils.

SINGLE NODE CONTROL

The first step in the control process is to create a method for matching the force from a single node to the wind tunnel forces. After the solution for one node is found, it can be extended to include multiple nodes.

This process is accomplished in 3 steps. In the first step, the desired force time history is converted to driving voltages for the electromagnet, specifying what coils are driven on and for what duration. A test run of the apparatus is then run, generating three arrays of data, the desired force from wind tunnel data (W), measured magnet force response (R), and actual commanded force (A). The results of this step are shown in Figure 4.

Step 2 involves two calculations, to determine the relationships between 1) R and A, and 2) W and A.

First, the magnet force is written as a function of the command voltage, its time derivative, and its integral

$$R = f\left(A, \dot{A}, \int A dt \right)$$

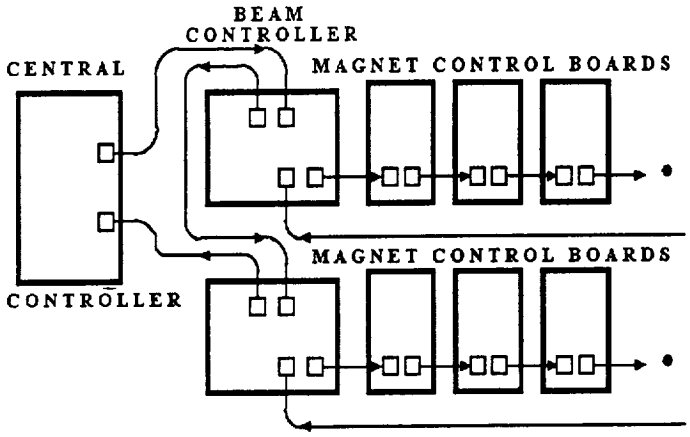

Figure 3 Schematic View of the Command Structure.

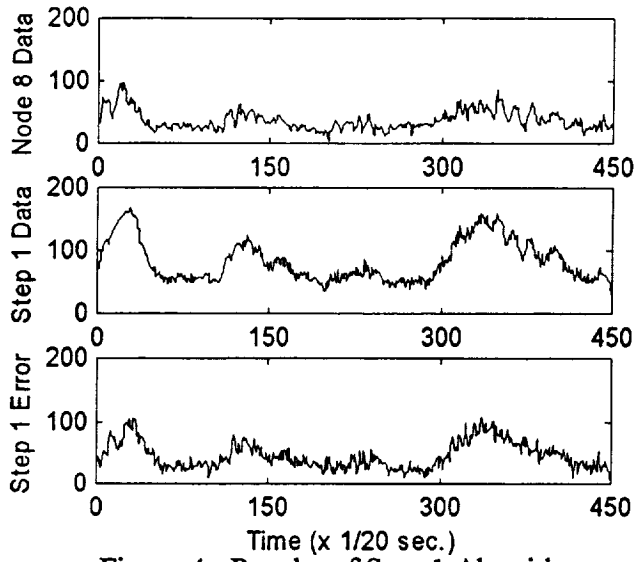

Figure 4. Results of Step 1 Algorithm

At time t_k we posit a relationship between magnet force and command voltage that can be written as a linear time-domain convolution

$$R_k = aA_k + bA_{k-1} + cA_{k-2} + \text{ϕ}$$

We can calculate optimal values of the constants a, b, c, ... by minimizing a performance measure J given by

$$J = \sum \left(aA_k + bA_{k-1} + cA_{k-2} + \text{ϕ} - R_k\right)^2$$

This implies

$$\frac{\partial J}{\partial a} = \frac{\partial J}{\partial b} = \text{ϕ} = 0$$

The derivatives of J are evaluated at each time in the time history, providing an overdetermined set of equations for the constants, which is solved using a least squares technique.

The second calculation in step 2 is used to enforce the requirement that R = W at all times t_i in the time history. We define a matrix M as

$$M = \begin{bmatrix} a & b & c & d & e & \text{ϕ} \\ 0 & a & b & c & d & \text{ϕ} \\ 0 & 0 & a & b & c & \text{ϕ} \\ 0 & 0 & 0 & a & b & \text{ϕ} \\ \text{ϑ} & \text{ϑ} & \text{ϑ} & \text{ϑ} & \text{ϑ} & \text{ϕ} \\ 0 & 0 & 0 & 0 & 0 & a \end{bmatrix}$$

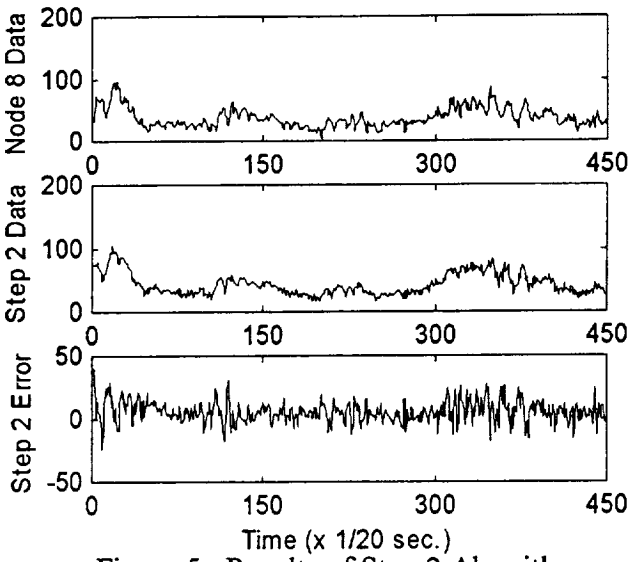

Figure 5. Results of Step 2 Algorithm

and define Wr as the row reversal of W_i, and likewise Ar as the row reversal of A_i. Solving the following equation

$$Ar = M^{-1}Wr$$

yields Ar. If Ar is then row reversed, the drive data for the magnet is obtained. Finally, a modified set of constants a, b, c, ... is computed as described above, and another cycle of the testing apparatus is performed. The results of the second calibration step are shown in Figure 5.

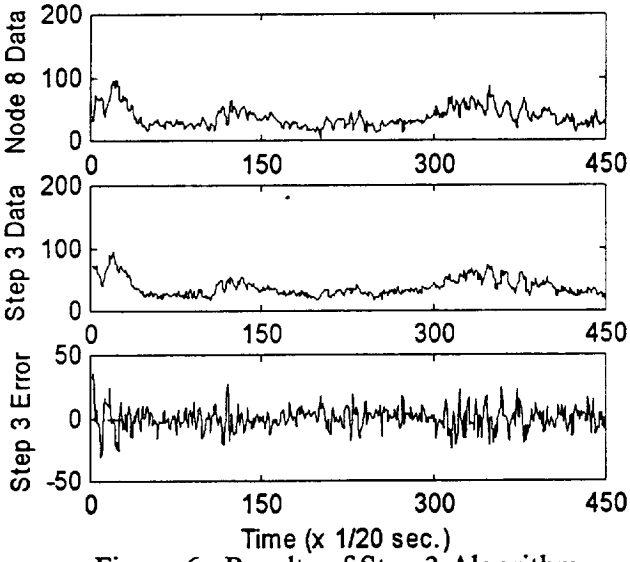

Figure 6. Results of Step 3 Algorithm

In the third and final calibration step, the peaks of the wind tunnel data are achieved. Another algorithm searches through the wind tunnel force data for significant changes between two adjacent samples. It then backs up no more than 20 points and increases their values to account for the magnet rise time. Once this step is completed, the algorithm in the first step is run again and a final cycle of the test apparatus is performed. The results of step 3 are shown in Figure 6.

MULTI-NODE CONTROL

The multi-magnet approach is similar to the single magnet approach, except that additional terms are added to account for the effects of the adjacent magnets. The procedure for four magnets is reflected in the equations:

$$R1 = f\left(A1, \dot{A1}, \int A1dt, W2, W3, W4\right)$$

$$R1_x = aA1_x + bA1_{x-1} + cA1_{x-2} + \varphi + rW2_x + sW3_x + tW4_x$$

$$J = \sum (aA1_x + bA1_{x-1} + cA1_{x-2} + \varphi - R1_x)^2$$

$$C = \begin{bmatrix} A1_1 & 0 & 0 & \varphi & W2_1 & W3_1 & W4_1 \\ A1_2 & A1_1 & 0 & \varphi & W2_2 & W3_2 & W4_2 \\ A1_3 & A1_2 & A1_1 & \varphi & W2_3 & W3_3 & W4_3 \\ \eth & \eth & \eth & \varphi & \eth & \eth & \eth \\ A1_n & A1_{n-1} & A1_{n-2} & \varphi & W2_n & W3_n & W4_n \end{bmatrix}$$

$$\begin{bmatrix} a \\ b \\ c \\ \eth \\ r \\ s \\ t \end{bmatrix} = (C^T C)^{-1} CR1$$

$$R1_x = W1_x$$

$$M = \begin{bmatrix} a & b & c & d & e & & r & s & t & \\ 0 & a & b & c & d & & 0 & r & s & \\ 0 & 0 & a & b & c & & 0 & 0 & t & \\ 0 & 0 & 0 & a & b & & 0 & 0 & 0 & \\ 0 & 0 & 0 & 0 & a & & 0 & 0 & 0 & \\ & & & & & \text{æ} & & & & \\ & & & & & & & & & \text{æ} \end{bmatrix}$$

$$A1r = M^{-1}(W1r - rW2r - sW3r - tW4r)$$

Finally, the drive data for *A1* magnet is obtained by row reversing *A1r*.

Figure 7 shows a comparison of the force induced in one magnet in the actuator array, and he target wind tunnel force time history. The degree of reproduction is considered to be outstanding for practical purposes of testing a full-scale metal roof.

CONCLUSION

The force exerted by an electromagnet on a thin metal roofing material is highly nonlinear with gap distance, and adjacent magnet nodes exhibit significant cross coupling. Full-scale metal roof ests require force profiles to match wind tunnel results, with all nodes synchronized to account for he spatial effects of high velocity winds. The approach described has proven capable of achieving he desired functions both temporally and spatially.

The techniques for adapting the actuator drive to accommodate the nonlinearity of gap listance and the influence of neighboring actuators are extremely effective and the mathematics are widely applicable to similar control problems involving coupling and nonlinearity. The actuators are possibly applicable to specialized applications such as dynamic loading, fatigue testing, etc.

One limitation of the technique is the offline processing required. Although it is conceivable hat this could be done in real-time, it was unnecessary for this application since the target trajectory vas known from the outset.

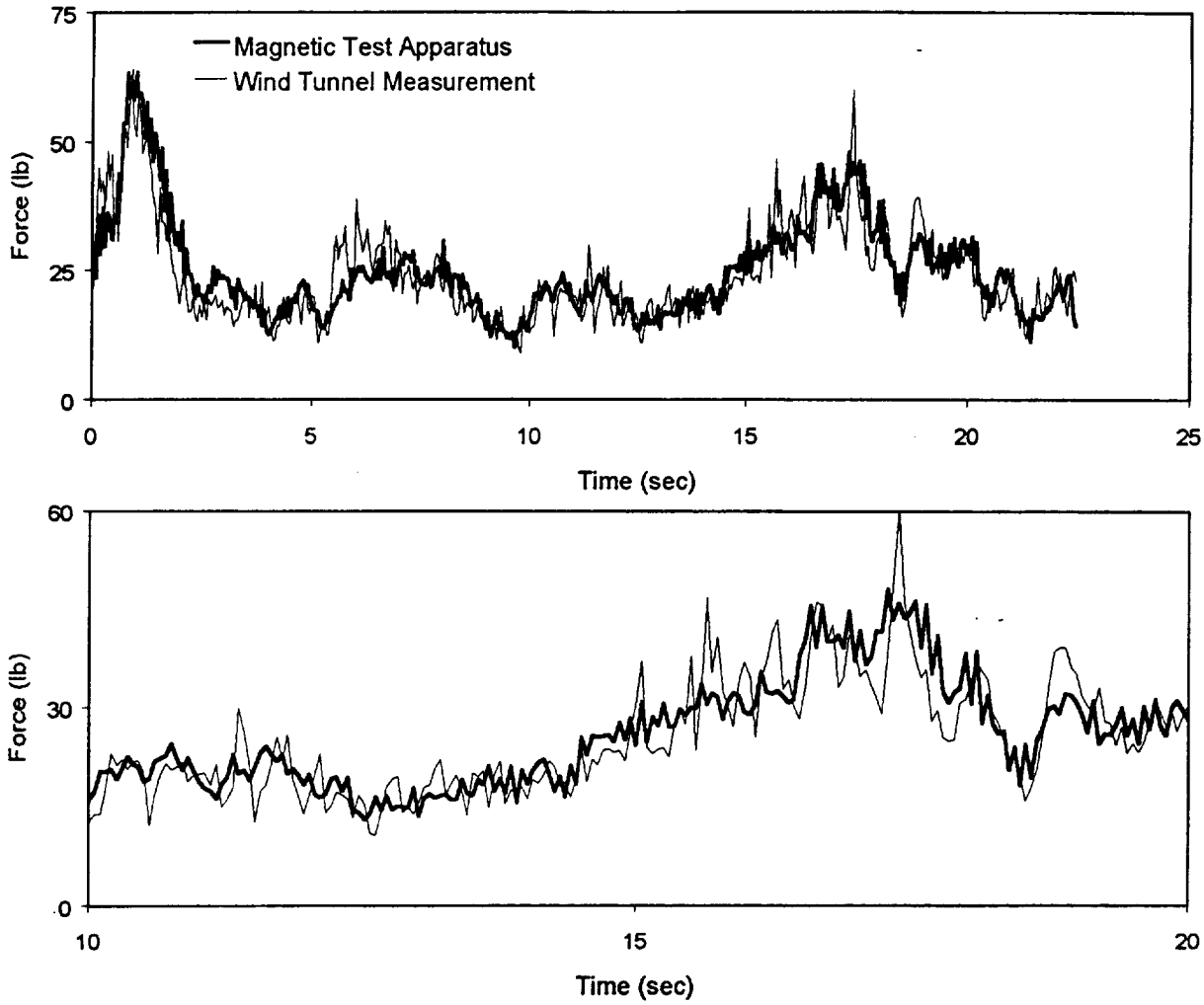

Figure 7. Comparison of Roof Forces Induced in Wind Tunnel and by Magnetic Test Apparatus

AKNOWLEDGEMENTS

The authors thank the Metal Building Manufacturers Association (MBMA), American Iron and Steel Institute (AISI) and the Metal Constructors Association (MCA) for providing the funding for this research. They also thank Tim Stults for his work on the electronics and structure; Robert Lewis for his work with the load cells; and Mark Maupin for his work on the structure.

REFERENCES

[1] K.C. Mehta and R. D. Marshall, *Guide to the Use of Wind Load Provisions of ASCE 7-95*, (Virginia: the American Society of Civil Engineers, 1998).

[2] D. Surry, T. C. E. Ho, and G. R. Lythe, Simulation Requirements for Roof Wind Loads Near the Corners of Low Buildings with Low-Slope Roofs, ASCE Structures Congress '99, New Orleans, LA, April 19-22, 1999.